Pulsed Pumping of Semiconductor Disk Lasers

Nils Hempler[1], John-Mark Hopkins[1], Alan J. Kemp[1], Nico Shultz[2], Marcel Rattunde[2], Joachim Wagner[2], Martin D. Dawson[1], David Burns[1]

[1]*Institute of Photonics, University of Strathclyde, Wolfson Centre, 106 Rottenrow, Glasgow, G4 0NW, Scotland, UK*
[2]*Fraunhofer Institut fuer Angewandte Festkoerperphysik, Tullastr. 72, 79108 Freiburg*

Abstract: Efficient operation of semiconductor disk lasers is demonstrated using uncooled and inexpensive 905nm high-power pulsed semiconductor pump lasers. Laser emission, with a peak power of 1.7W, is obtained from a 2.3μm semiconductor disk laser. This is seven times the power achieved under continuous pumping. Analysis of the time-dependent spectral characteristics of the laser demonstrate that significant device heating occurs over the 100-200ns duration of the pumping pulse - finite element modelling of the thermal processes is undertaken in support of these data. Spectral narrowing to below 0.8nm is obtained by using an intra-cavity birefringent filter.

OCIS codes: (140.5960) Semiconductor lasers; (140.5560) Pumping; (140.3480) Lasers, diode-pumped; (140.6910) Thermal effects.

References and links

1. M. Kuznetsov, F. Hakimi, R. Sprague, and A. Mooradian, "Design and characteristics of high-power (> 0.5-W CW) diode- pumped vertical-external-cavity surface-emitting semiconductor lasers with circular TEM_{00} beams," IEEE J. Sel. Top. Quantum Electron. 5, 561-573 (1999)
2. A.V. Shchegrov, D. Lee, J.P. Watson, A. Umbrasas, E.M. Strzelecka, M.K. Liebman, C.A. Amsden, A. Lewis, V.V. Doan, B.D. Moran, J.G. McInerney, A. Mooradian, "490-nm coherent emission by intracavity frequency doubling of extended cavity surface-emitting diode lasers," Proc. SPIE, vol. 4994, p. 197 (2003).
3. J.P. Watson, A.V. Shchegrov, A. Umbrasas, D. Lee, C.A. Amsden, W. Ha, G.P. Carey, V.V. Doan, A. Lewis, A. Mooradian, "Laser sources at 460 nm based on intracavity doubling of extended-cavity surface-emitting lasers" Proc. SPIE, vol. 5364, p. 116 (2004)
4. J.-M. Hopkins, S. Calvez, A. J. Kemp, J. E. Hastie, S. A. Smith, A. J. Maclean, D. Burns, M. D. Dawson., "High-power vertical external-cavity surface-emitting lasers", Physica Status Solidi (c), 3, 380, (2006).
5. A. Ouvrard, A. Garnache, L. Cerutti, F. Genty, D. Romanini, "Single-Frequency Tunable Sb-Based VCSELs Emitting at 2.3 μm". IEEE Photon. Tech. Lett, Vol. 17, pp2020-2022, (2005)
6. J. Hastie, S. Calvez, M. Dawson, T. Leinonen, A. Laakso, J. Lyytikäinen, and M. Pessa, "High power CW red VECSEL with linearly polarized TEM_{00} output beam," Opt. Express 13, 77-81 (2005)
7. J. M. Hopkins, S. A. Smith, C. W. Jeon, H. D. Sun, D. Burns, S. Calvez, M. D. Dawson, T. Jouhti, and M. Pessa, "0.6 W CW GaInNAs vertical external-cavity surface emitting laser operating at 1.32 μm," Electron. Lett. 40, 30-31 (2004)
8. N. Schulz, M. Rattunde, C. Manz, K. Koehler, C. Wild, J. Wagner, S.-S. Beyertt, U. Brauch, T. Kuebler, and A. Giesen, "Optically Pumped GaSb-Based VECSEL Emitting 0.6 W at 2.3 μm," IEEE Photonics Technol. Lett. 18, 1070-1072 (2006)
9. J.-M. Hopkins, A. J. Maclean, D. Burns, N. Schulz, M. Rattunde, C. Manz, K. Koehler, and J. Wagner, "Tunable, Single-frequency, Diode-pumped 2.3μm VECSEL," presented at Conference on Lasers and Electro-Optics, (Long Beach, 2006)
10. S. Hoogland, S. Dhanjal, A.C. Tropper, J.S. Roberts, R. Haring, R. Paschotta, F. Morier-Genoud, U. Keller, "Passively Mode-Locked Diode-Pumped Surface-Emitting Semiconductor Laser," IEEE Photon. Tech. Lett. 12, 1135-1137 (2000).
11. J. L. Chilla, S. D. Butterworth, A. Zeitschel, J.P. Charles, A. L. Caprara, M. K. Reed, and L. Spinelli, "High power optically pumped semiconductor lasers," in Solid State Lasers XIII: Technology and Devices, R. Scheps, and H. J. Hoffman, eds., Proc. SPIE 5332, 143-150 (2004)
12. Z. L. Liau, "Semiconductor wafer bonding via liquid capillarity," Appl. Phys. Lett. 77, 651-653 (2000)
13. F. van Loon, A. J. Kemp, A. J. Maclean, S. Calvez, J. -M. Hopkins, J. E. Hastie, M. D. Dawson, and D. Burns, "Intracavity diamond heatspreaders in lasers: the effects of birefringence," Opt. Express 14, 9250-9260 (2006)

14. A. J. Kemp, G. J. Valentine, J. M. Hopkins, J. E. Hastie, S. A. Smith, S. Calvez, M. D. Dawson, and D. Burns, "Thermal management in vertical-external-cavity surface-emitting lasers: Finite-element analysis of a heatspreader approach," IEEE J. Quantum Electron. 41, 148-155 (2005)
15. A. Härkönen, M. Guina, O. Okhotnikov, K. Rößner, M. Hümmer, T. Lehnhardt, M. Müller, A. Forchel, M. Fischer, "1-W antimonide-based vertical external cavity surface emitting laser operating at 2-µm",Optics Express, Vol. 14, Issue 14, pp. 6479-6484, (2006)
16. Li Fan, Mahmoud Fallahi, Jörg Hader, Aramais R. Zakharian, Jerome V. Moloney, James T. Murray, Robert Bedford, Wolfgang Stolz, and Stephan W. Koch, Multichip vertical-external-cavity surface-emitting lasers: a coherent power scaling scheme, , Optics Letters, Vol. 31, Issue 24, pp. 3612-3614 (2006)
17. Esa J. Saarinen, Antti Härkönen, Soile Suomalainen, and Oleg G. Okhotnikov, Power scalable semiconductor disk laser using multiple gain cavity, Optics Express, Vol. 14, Issue 26, pp. 12868-12871 (2006)
18. K.W. Su, S.C. Huang, A. Li, S.C. Liu, Y.F. Chen, and K.F. Huang, "High-peak-power AlGaInAs quantum-well 1.3µm laser pumped by a diode-pumped actively *Q*-switched solid-state laser", Opt.Letters Vol.31, No.13, 2009-2011 (2006)
19. for full detail see www.osram-os.com
20. for full detail see www.perkinelmer.com
21. Dr Heller Elektronik KG, Germany
22. K. S. Kim, J. R. Yoo, S. H. Cho, S. M. Lee, S. J. Lim, J. Y. Kim, J. H. Lee, T. Kim, Y. J. Park, "1060 nm vertical-external-cavity surface-emitting lasers with an optical-to-optical efficiency of 44% at room temperature", Appl. Phys. Lett. 88, 091107 (2006)
23. Hans Lindberg, Martin Strassner, Eckart Gerster, Jorgen Bengtsson, Anders Larsson, Thermal Management of Optically Pumped Long-Wavelength InP-Based Semiconductor Disk Lasers, IEEE Journal of Selected Topics in Quantum Electronics, 11, 1126, (2005)
24. T. Borca-Tasciuc' D. W. Song, J. R. Meyer, I. Vurgaftman, M.-J. Yang, B. Z. Nosho, L. J. Whitman, H. Lee and R. U. Martinelli, G. W. Turner, M. J. Manfra, G. Chen, Thermal conductivity of $AlAs_{0.07}Sb_{0.93}$ and $Al_{0.9}Ga_{0.1}As_{0.07}Sb_{0.93}$ alloys and $(AlAs)_1/(AlSb)_{11}$ digital-alloy superlattices, *Journal of Applied Physics*, 92, 4994, (2002)
25. S. Adachi, Optical dispersion relations for GaP, GaAs, GaSb, InP, InAs, InSb, $Al_xGa_{1-x}As$, and $In_{1-x}Ga_xAs_yP_{1-y}$, *Journal of Applied Physics*, 66, 6030, 1989
26. "Electronic Archive: New Semiconductor Materials, Characteristics and Properties," Ioffe Physico-Technical Institute, 2003
27. M. Muñoz, T.M. Holden, F.H. Pollak, M. Kahn, D. Ritter, L. Kronik , G.M. Cohen, Optical constants of $In_{0.53}Ga_{0.47}As$/InP: Experiment and modelling, *Journal of Applied Physics*, 87, 1780, (2000)
28. Element 6, "Diamond Types," (Element 6 Ltd., 2006)

1. Introduction

In recent years, the semiconductor disk laser [1] has received considerable interest due to its potential for use in applications ranging from gas laser replacement [2] and laser light projection [3] through to free-space optical communications [4] and sensing [5]. Operation at wavelengths spanning 670-2400nm has been demonstrated [6-8], and output powers of many tens of watts have been produced around 1µm. Furthermore, a wide range of functionality, such as narrow line-width and modelocked operation has been demonstrated [9]. The ability to wavelength engineer semiconductor disk lasers, as well as to realise a wide range of modes of operation, makes this laser format particularly attractive.

Similar to most other solid-state lasers, the performance of semiconductor disk lasers is limited by the heating induced in the gain medium due to pumping; however, in this case it is the absolute temperature rise that must be controlled. To address this issue, two distinct thermal management techniques have evolved: substrate removal and bonding to a high conductivity heat sink [11], or the use of a high conductivity transparent heat-spreader bonded on top of the disk [12,13]. The first technique requires intensive post-processing of the device and is much less effective when the thermal impedance of the integrated mirror is large. The latter requires very accurate bonding and introduces an additional intra-cavity element, and so, increased laser losses. However, it provides superior thermal management [14] for the low thermal conductivity semiconductor materials required for a 2.3µm semiconductor disk laser [8, 15]. Another emerging technique – the use of multiple gain

elements – is becoming an increasing popular means to bypass the limiting effects of device heating [16,17].

This paper investigates the potential for increasing the output powers obtainable from semiconductor disk lasers by using pulsed or quasi-CW pumping to minimise device heating. The implications for device performance, along with the benefits for applications, will also be discussed.

2. The Pump Laser

Previous pulsed pumping of semiconductor disk (SD) lasers used the output from a Q-switched Nd:YAG laser producing pulses of around 10ns [18] – these results suggested that the device heating was small, as the SD laser output closely tracked the pump pulse. These investigations were, however, largely focussed on the materials and structural development of the active disk: improving the optical characteristics in the absence of problematic thermal effects. This paper describes the performance of pulsed SD lasers with an eye to applications. In this regard, a bulk solid-state laser is not an appropriate pump source. However, high-power pulsed semiconductor lasers have recently become available at low cost – e.g. from OSRAM [19] and Perkin-Elmer [20]. Throughout this work, the OSRAM SPL PL90_3, 75W nanostack laser device was used.

The basic characteristics of the SPL PL90_3 when driven with a commercially available avalanche transistor circuit [21] are shown in figure 1. The output pulse duration could be adjusted from ~15 – 180ns and the repetition frequency was variable over ~1-10kHz. In these experiments, a typical pulse duration and frequency of ~180ns and 1kHz respectively were used. No cooling was required for this pump unit (see layout detailed in figure 2).

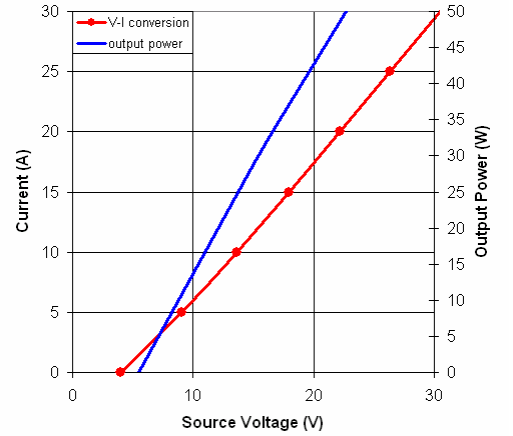

Fig.1. Output characteristics of OSRAM SPL Pl90_3 pulsed laser as a function of voltage applied to the avalanche transistor driver circuit

Fig. 2. Compact high-power pulsed pump laser (SPL PL90_3) and avalanche transistor driver configuration.

The pump laser, emitting at 905nm, was collimated then focussed into a 100µm core optical fibre using two x10 microscope objectives. A f=150mm cylindrical lens was positioned between the two lenses to compensate for the astigmatism of the laser source. The coupling efficiency into the optical fibre was around 55% – this could be significantly increased by using more appropriate coupling optics, or a larger core optical fibre.

3. Pulsed Pumping of a 2.3µm Semiconductor Disk Laser

To investigate pulsed (or quasi-cw) pumping of semiconductor disks lasers, the output from the optical fibre was coupled to the disk laser configuration shown schematically in figure 3. A sequence of two lens (f=14.5mm triplet and f=11mm aspheric) was used to illuminate an approximately 80x110µm spot area on the surface of the disk. The disk featured a highly reflecting mirror centred on 2.3µm consisting of 21.5 layer pairs of AlAsSb/GaSb. The gain was provided by ten 10-nm-thick $Ga_{0.69}In_{0.31}As_{0.07}Sb_{0.93}$ quantum wells positioned appropriately at the anti-nodes of the optical field. Full details of this type of semiconductor disk laser can be found in reference 15. A 50mm radius of curvature mirror having a reflectivity of 97% terminated the cavity and was used as the laser output coupler. The cavity length producing the maximum output power was found to be ~44mm, which, by way of an ABCD analysis, corresponded to a laser mode radius of ~110µm at the active disk. The semiconductor disk was capillary bonded to a 0.5mm thick diamond heatspreader (see reference 12 and 13) – this was done to permit the scaling of the output power under continuous wave pumping, and was undertaken prior to pulsed pumping investigations. The effect of the heatspreader is somewhat different under pulsed pumping and this is discussed more fully in the finite element analysis section later.

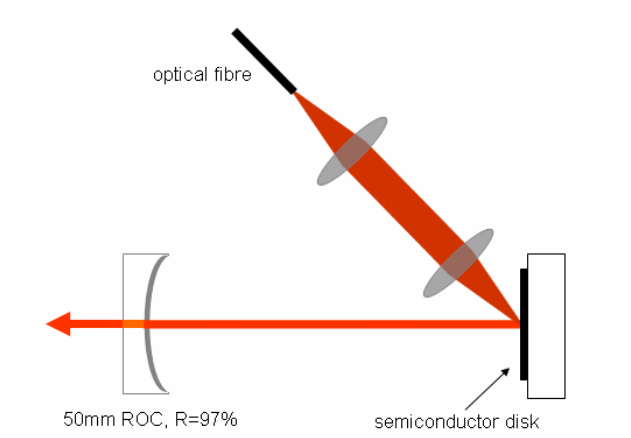

Fig. 3. Optically pumped semiconductor laser configuration – the GaAsSb disk laser emits at 2.3µm

The pulse waveforms of the incident pump laser operating with a source voltage of 20V, and the output from the disk laser are shown in figure 4. The pump and laser FWHM pulse-widths were 179 and 156ns respectively and the turn-on delay of the laser was measured as ~24ns. [It should be noted that the response times of the photodetectors used (InGaAs for the 905nm pump, and extended InGaAs for the 2.3µm laser) are significantly different – the mid-IR detector being unable to fully resolve the rise and fall times of the pulse. The ring-down time of the laser cavity cannot therefore be resolved. This does not, however, limit the investigation of pulsed pumped disk lasers in general. The output pulse from the disk laser closely mirrors the shape of the pump laser pulse apart from perhaps a slight decrease in power at the end of the pulse – the laser pulse shape, however, varied somewhat with cavity alignment, so care must be taken in drawing conclusions with respect to device heating from

the small variations in these data. It is clear though that the temporal profile of the output pulse from the disk laser is not significantly affected by device heating.

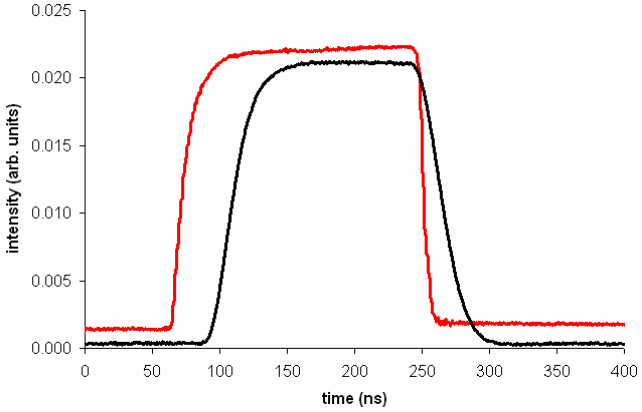

Fig. 4. Pump (top trace) and output laser (bottom trace) waveforms - source voltage of 20V; 100µm core fibre coupling. Note: an intensity offset between the two traces has been introduced for clarity.

Measurements of the incident pump power and the corresponding output power from the disk laser are plotted in figure 5. The powers quoted were calculated from a measurement of the average power and the duty cycle of the pulse train. In other words, the measurement refers to the *on-time* power since both pump and laser pulses are effectively square. Also plotted in figure 5 are the corresponding room temperature continuous-wave (cw) pumping data for the same laser set-up for direct comparison. [The semiconductor disk in the cw pumped laser was held at 20°C by a closed-loop water circuit; however, for the pulsed laser, no active cooling was used for either the pump laser or the semiconductor disk.] It is clear that thermally-induced rollover significantly affects the performance of the cw pumping case; however, pulsed pumping allows much higher output powers to be obtained – approximately 7 times more in this case. A reduction in the slope efficiency of the pulsed data is evident at output powers around 1.2W, indicating that pump induced heating may be starting to affect the performance. At the highest pump powers used (~40W), output powers of well over 2W would be expected from an extrapolation of the linear part of the laser characteristic; however, a maximum power of only 1.7W was measured.

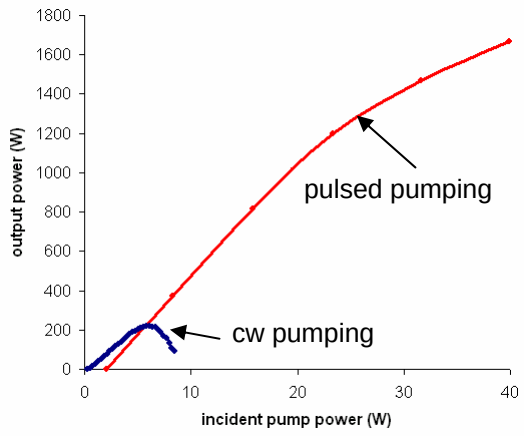

Fig. 5. Power transfer characteristic of the 2.3µm semiconductor disk laser for both room temperature continuous wave and pulsed pumping

As in the cw case, pump-induced heating is the obvious candidate for this drop in device efficiency; however, it is noteworthy that no significant change in the pulse profiles was observed, even at the highest powers. Furthermore, the qualitative form of the 'thermal rollover' is softer and less sudden under pulsed pumping than for cw pumping. Additionally, it should be noted that the difference in the pulsed and cw pumping wavelengths (905 and 980nm) result in about a 5% difference in the fractional pump heating. The pulsed pumping case is therefore disadvantaged to this degree on direct comparison using the data in figure 5.

Pulsed pumping can significantly enhance the on-time output power obtainable from semiconductor disk lasers by minimising the effects of pump induced heating, and hence reducing the detuning of the peak gain wavelength from the micro-cavity resonance of the disk (detailed later in figure 9). This technique limits the operating time of the laser to the order of a few hundred nanoseconds, and this, of course, will have consequences for applications. In principle, however, a wide range of applications, and specifically sensing, are suited to the enhanced on-time powers and short pulse durations of pulsed pumped semiconductor disk lasers. The high peak power serves to enhance system sensitivity and the repetitively pulses are suited to lock-in detection techniques. So, if a pulsed pumped source is applicable, significant power enhancements can be offered – in an inexpensive, very compact and uncooled unit.

4. Spectral Analysis of Output Laser Pulses

In order to characterise the spectral evolution of the output pulses, the output from the semiconductor disk laser for an incident power of ~30W, was assessed using a grating monochromator. By optimising the focussing onto the spectrometer and using 50μm slits, the longitudinal mode groups [22] associated with the etalon formed by the diamond heatspreader could be fully resolved. The temporal development of each of the eleven mode groups that reached threshold is plotted in figure 6. Each mode group was numbered from 1 to 11, low group numbers appearing early in the pulse and high numbers later. By manipulating these data, a measure of the *quasi-instantaneous* spectrum of the laser as time progresses can be obtained, and a subset of these data are shown in figure 7.

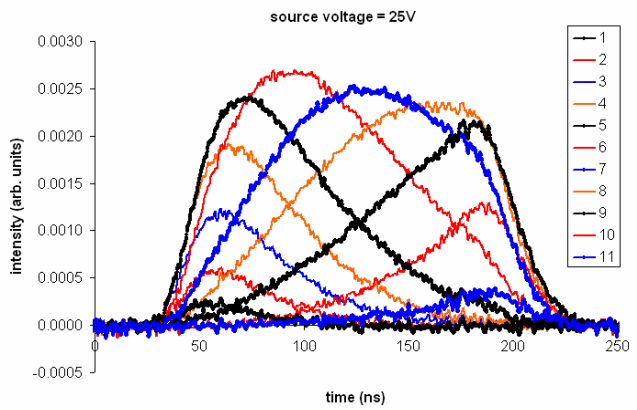

Fig. 6. Temporal dependence of the 11 'diamond etalon' modes of the semiconductor disk laser. The source voltage applied to the pulsing circuit was 25V – incident pump power ~31W

A clear red-shift (from 2289nm to 2306.5nm) with respect to time can be seen throughout the duration of the disk laser pulse. Again, much like in the power analysis previously, this is an indication that the device is heating. So, from measurements of the peak of the instantaneous spectra and by using the measured rate of change of the photoluminescence peak with temperatures (in the range 260-300K) of ~0.33nm/K, the time dependent change in device temperature can be mapped. Figure 8 records the measured spectral shift and the

corresponding temperature data as a function of time during the laser pulse. The implied temperature rise was therefore ~53K and so the heating rate was 0.35K/ns for the case considered here. Assuming a linear change in device heating by pumping, the 24ns delay to the onset of laser oscillation will add a further 9K to the maximum temperature making this value ~62K.

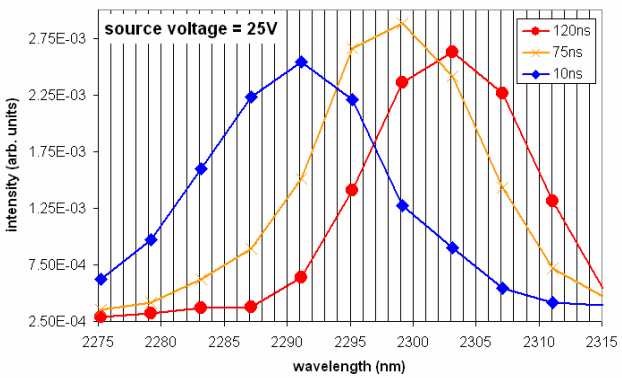

Fig. 7. Instantaneous oscillation spectrum of the pulse pumped semiconductor disk laser at various times throughout the output laser pulse. The spectrum shifts to longer wavelengths with time – i.e. the temperature of the device increases.

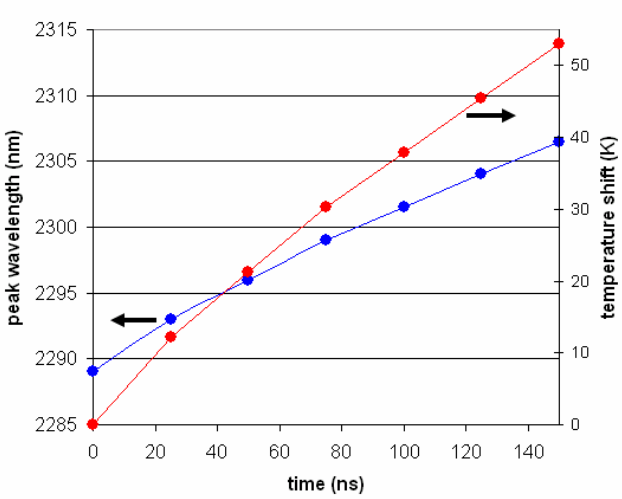

Figure 8. Spectral shift of the instantaneous oscillation spectrum versus time after turn on of the output pulse. The temperature shift implied by these data is also plotted – 0.33nm/K was assumed for the disk laser resonance shift with temperature.

The temperature characteristics of semiconductor disk lasers which do not exploit heatspreaders will of course have significantly different spectral characteristics throughout the duration of the output pulse. Typically disk lasers without heatspreaders will only feature one mode cluster (often this contains only one longitudinal mode, but more frequently many oscillate and the bandwidth is a fraction of a nanometre). For similar operating conditions to those used here, such a single mode cluster would, however, be subject to a similar spectral shift due to device heating.

To stabilise the spectral behaviour of the pulsed disk laser, some form of optical filter is necessary – to this end, a 2mm thick quartz birefringent filter was inserted into the disk laser cavity and oriented at Brewster's angle to minimise the loss. Oscillation on a selected mode cluster (of bandwidth, $\Delta\lambda < 0.8$nm) resulted throughout the full duration of the output pulse –

the duration of which was slightly reduced to 150ns. The output pulse profile was very similar to those presented in figure 4 - the increased turn-on delay reflects the reduced gain present at the operating wavelength at low temperatures (i.e. the beginning of the pulse); however, as the device heats, the laser oscillation progresses as before, but fixed at the wavelength band defined by the intra-cavity filter. There was some evidence of an output wavelength shift within this reduced bandwidth; however, the resolution of the monochromator was insufficient for accurate measurements to be made. The analysis of this chirp and the prospects for stabilised single-frequency operation will be the subject of a future paper.

5. Pulsed Disk Laser without Heatspreader

With the heatspreader removed, the power characteristics remained essentially the same as before; however, since there are no intra-cavity etalon effects due to the diamond heatspreader, the oscillating wavelength band is not modulated. Extracting the data is therefore not so straightforward; however, visual assessment indicated a spectral shift of approximately 16nm over the duration of the pulse, with shorter wavelengths being emitted early and longer wavelengths later as the device heats. Backlash in the micrometer drive to the monochromator made relative wavelength measurement less accurate than for the device with the heatspreader; however, observations implied a fairly smooth wavelength shift versus time across the pulse. Further work with a more appropriate spectrometer is therefore required to fully characterise the wavelength shift during the pulse.

On insertion of the 2mm birefringent filter, the output spectrum consisted of only one mode cluster which had a 0.8nm bandwidth, i.e. the same width as each of the etalon mode clusters in the case with the heatspreader attached. By adding a thicker BRF, or indeed an etalon, this bandwidth would be expected to be further reduced. The output pulse duration at 25V source voltage applied to the pulsing circuit (~30W incident peak pump power) was ~152ns, indicating that similar pumping conditions were present with and without the heatspreader; the reduced pump reflectivity (i.e. higher pumping efficiency) of the former being balanced by the reduced intra-cavity loss of the latter.

The semiconductor disk laser operated under conditions of strong pulsed pumping can therefore operate as a swept wavelength source or a fixed, narrow-band source depending on the nature of the intra-cavity filter that is used. Also, the behaviour of the system with and without a heatspreader is effectively the same, apart from the pixilation of the output spectrum that is introduced as a consequence of the heatspreader acting as a thin etalon.

6. Thermal Characteristics of Semiconductor Disk Lasers

The spectral behaviour of the semiconductor disk laser is predominantly determined by the relationship between the gain spectrum of the quantum wells making up the gain region of the device and the resonant effects of the chip micro-cavity (see figure 9). One mirror of the micro-cavity arises from the Fresnel reflection due to the large refractive index mismatch at the semiconductor / air interface, the other being the DBR of the disk. The quantum wells are placed at the anti-nodes of the optical field inside this micro-cavity to maximise the device gain – an effect referred to as *resonant periodic gain* or RPG [1].

A so-called *resonant* semiconductor disk is designed with a micro-cavity length such that at the resonant optical enhancement wavelength, the field anti-nodes coincide with the quantum wells. The observed gain is therefore modified by the micro-cavity – i.e. it is enhanced but reduced in bandwidth. [An anti-resonant disk has its quantum wells shifted by a quarter wavelength with respect to the resonant device – in this way, the gain spectrum remains unmodified; however, the magnitude of the gain is not enhanced.] As a result, the spectral properties of a *resonant* disk are intimately linked to the micro-cavity resonance; however, the temperature dependences of the micro-cavity resonance and the quantum wells are usually significantly different.

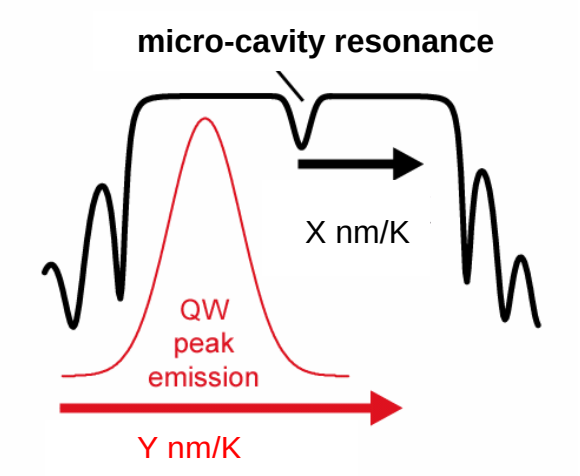

Figure 9. Schematic of the reflectivity function of the semiconductor disk laser showing the position of the micro-cavity resonance (within which the laser oscillation is constrained), and the gain spectrum of the quantum wells. These two functions shift to longer wavelengths as temperature increases but at different rates (Y>X). When the two functions coincide, the device efficiency is maximised - further temperature increases lead to reduced performance.

For the 2.3µm disk lasers used here, the temperature dependences of the micro-cavity resonance and the quantum well gain are ~+0.33nm/K and +1nm/K respectively. Therefore, as temperature increases, the quantum well gain *walks away* from the micro-cavity resonance, see figure 9 – this is reflected in a reduction in laser efficiency, output power rollover, and / or eventual oscillation quenching (as evidenced in figure 5 for the cw pumping case). Typically, in an attempt to counteract this effect, the disk laser design incorporates a spectral offset between the gain and micro-cavity resonance peaks such that at a given temperature they become aligned and the performance becomes optimal – this however, is no real substitute for appropriate thermal management.

7. Finite element analysis

In most pulse-pumped solid-state lasers, thermal changes take place on micro- or millisecond timescales. By contrast, the experimental evidence suggests that significant temperature changes occur on a nanosecond timescale in the semiconductor disk laser. In order to assess the thermal response of the device due to pulsed pumping, finite element thermal analysis was undertaken. The complexity of the model was reduced by assuming axial symmetry and grouping layers with similar thermal properties [14, 23]. The material properties were obtained by interpolation from the data in [24-28].

If an on-time incident pump power of 30W is assumed in a pump spot radius of 45µm, with a pulse duration of 180ns, finite element analysis predicts the temperature variation presented in figure 10. The temperature changes with and without a diamond heatspreader are presented, and the experimental data is provided for comparison. The temperature varies spatially within the device, and hence a weighted average has been used:

$$T_{ave} = \frac{\int T(r,z).I_p(r).dV}{\int I_p(r).dV} \qquad (1)$$

Where, $I_p(r)$ is the radial variation of the pump mode and hence, approximately, of the gain. The integration is over the section of the device that provides gain. A constant offset has been applied to the experimental data to account for the heating of the device that occurs before the laser oscillation builds up.

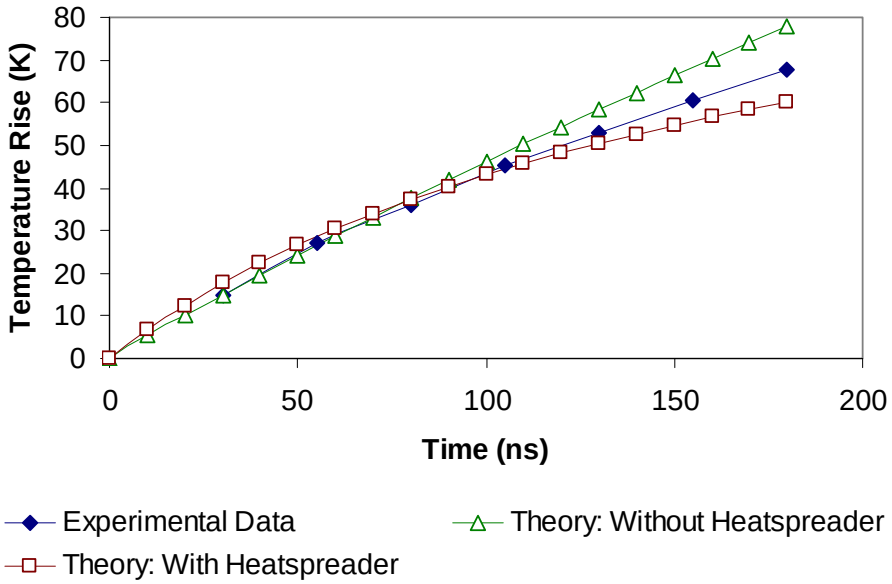

Figure 10. Time-dependent heating of a GaSb-based semiconductor disk laser predicted by finite element analysis and compared to the experimental data. A pump pulse of 180ns with an on-time incident power of 30W, and a pump spot radius of 45μm are assumed. A weighted average of the temperature is taken to account for the spatial variation.

As figure 10 illustrates, heating is indeed predicted to occur on nanosecond timescales. This is because the volume being heated is very small – a disk 45μm in radius by about 1μm thick, due to the very short pump-absorption length. The magnitude of the temperature change is in reasonable agreement with the experimental data. In addition, the temperature changes with and without the heatspreader in place are predicted to be broadly similar, again in line with experimental observations. The reduction in the temperature rise in the case where a heatspreader is present is due to the high thermal conductivity and heat capacity of the diamond.

As the finite element analysis illustrates, rapid temperature rises can occur in these lasers under nanosecond pulsed pumping, explaining the wavelength chirp observed experimentally. This is in sharp contrast to quasi-CW pumping of conventional diode-pumped solid-state lasers.

8. Conclusions

A new approach to pumping semiconductor disk lasers has been presented – quasi-cw pumping using uncooled high-power semiconductor lasers. In this way, 150ns duration approximately square-shaped pulses with peak power levels of ~1.7W have been obtained from a 2.3μm GaSb-based disk laser. Even though the average pump power level is rather low (a few mW), a reduction in efficiency at the highest pump powers suggests significant device heating. On closer analysis of the spectral behaviour of the disk laser output, the device heating was estimated to be of the order of 50-60K over the pump pulse duration of 180ns. A finite element model of this system supported these data; however, the detailed implications of this model require further study.

Under free-running operating conditions, the disk laser produced a substantial sweep in emission wavelength during the output pulse. After inclusion of a birefringent filter, this wavelength sweep could be significantly reduced to the resolution limit of the measurement apparatus. It is envisaged that further bandwidth reductions are possible, and the prospect of a compact, reliable, narrow-linewidth laser suitable for remote sensing is clear.